APPLICATION OF ARTIFICIAL NEURAL NETWORK IN PREDICTING THE ACTUAL MAXIMUM STRESS IN THE TUNGSTEN INERT GAS WELDMENT

BY

AGHO ETINOSA PROSPER

ENG2002336

DEPARTMENT OF INDUSTRIAL ENGINEERING,

FACULTY OF ENGINEERING

UNIVERSITY OF BENIN, BENIN CITY.

SEPTEMBER, 2025

APPLICATION OF ARTIFICIAL NEURAL NETWORK IN PREDICTING THE ACTUAL MAXIMUM STRESS IN TUNGSTEN INERT GAS WELDMENT.

BY

AGHO ETINOSA PROSPER

ENG2002336

A RESEARCH PROJECT WRITTEN AND SUBMITTED TO THE DEPARTMENT OF INDUSTRIAL ENGINEERING, FACULTY OF ENGINEERING, UNIVERSITY OF BENIN, IN PARTIAL FULFILMENT OF THE REQUIREMENTS FOR DEGREE OF BACHELOR OF ENGINEERING OF THE UNIVERSITY OF BENIN, BENIN CITY

OCTOBER, 2025

DECLARATION

I declare that:

This project work is based on a study undertaken by me in the Department of Industrial Engineering, University of Benin under the supervision of Engr. Dr. B.O ERHUNMWUNSE. This work has not been previously submitted for award of a degree elsewhere.

_____

Agho Etinosa Prosper

DATE: _____

CERTIFICATION

This is to certify that this project work titled "APPLICATION OF ARTIFICIAL NEURAL NETWORK IN PREDICTING THE ACTUAL MAXIMUM STRESS IN A TUNGSTEN INERT GAS WELDMENT" was carried out by AGHO ETINOSA PROSPER with the Matriculation Number ENG2002336, in the Department of Industrial Engineering, Faculty of Engineering, University of Benin, under my supervision.

_____ _____

Engr. Dr. B.O ERHUNMWUNSE DATE

Project supervisor

_____ _____

Engr Dr. (Mrs) I. C ILOUBE DATE

Project coordinator

_____ _____

Engr.Prof. P.E. AMIOLEMHEN DATE

Head of Department of Production Engineering

DEDICATION

This project is dedicated to my God almighty, my parents and all those who supported me from the beginning to this point. It is my prayer that God in his infinite mercy grants you your heart desires. Amen.

ACKNOWLEDGEMENTS

I am Extremely grateful to God Almighty for the success of this project work, for the grace to see this day and the grace to go through this course with good health and sound mind.

I want to appreciate my supervisor Engr. Dr. B.O ERHUNMWUNSE, for his support, patience, assistance and guidance in ensuring the success of my research work. May God bless you abundantly, sir.

I also love to appreciate the H.O.D of my department Prof. P.E AMIOLEMHEN and all staff for their respective contribution and effort towards the growth of this department, I pray the lord bless you and attend to all your needs.

I would also like to express my profound gratitude to my wonderful family - my parents Mr. and Mrs. E. AGHO, for their sponsorship, and prayers always. I also wish to express gratitude to my siblings - Praise, Perfect and confidence, to my wonderful friends and well wishers, to my pastor and close relative, I say a big thank you for all you've done for me and may the Good lord reach out to you in your point of needs and bless you.

I also appreciate my father, Engr. Dr. N.H. Osadiaye for always looking after me. May the Good lord bless you abundantly in jesus name.

TABLE OF CONTENTS

LIST OF FIGURES

LIST OF TABES

ABSTRACT

Welding is a vital manufacturing process used in several industries, including aerospace, automotive, and construction. However, residual and induced stresses that develop during welding due to rapid heating and cooling cycles often affect the structural integrity of the weldment thereby reducing the integrity of the structure. The study investigates the application of Artificial Neural Networks (ANN) in predicting the actual maximum stress in Tungsten Inert Gas (TIG) weldments and develop a predictive model capable of accurately estimating the actual maximum stress in TIG welded joints based on key process parameters such as welding current, voltage, and gas flow rate.

Twenty (20) experimental runs as generated by the Central Composite Design (CCD) was used to carry out TIG welding on mild steel plates. A Universal Stress Testing Machine was used to measure the actual maximum stress in the weldment and the result was recorded for each experimental run. This experimental result was then analyzed using ANN.

ANN trained trained the neural network with fourteen (14) of the observations and use three for network validation and another three for network testing. The best validation performance value of 80.6689 was observed at epoch 5 with an overall performance value of 0.96864. ANN predicted response values was compared with the experimental result and it showed a meritorious correlation with the experimental result trend.

The results revealed that the developed ANN model achieved high prediction accuracy with minimal error, confirming its capability to learn and represent the complex nonlinear relationship between the welding input parameters and the resulting actual maximum stress.

CHAPTER ONE

INTRODUCTION

1.1 Background To The Study

Welding is a crucial fabrication process widely used in manufacturing and construction industries to join materials, typically metals, by applying heat and pressure. Among the various welding techniques, Tungsten Inert Gas (TIG) welding, also known as Gas Tungsten Arc Welding (GTAW), is renowned for producing high-quality, precise welds with excellent mechanical properties. TIG welding utilizes a non-consumable tungsten electrode and an inert shielding gas, typically argon, to protect the weld area from atmospheric contamination, making it suitable for welding thin sections of stainless steel and non-ferrous metals such as aluminum and copper alloys (Kalpakjian and Schmid, 2014). The TIG welding process inherently introduces residual stresses into the welded structure due to the localized heating and rapid cooling of the metal. These residual stresses, induced during the welding thermal cycle, can lead to distortion, cracking, and reduction in the mechanical performance of the welded joint (Sindo and Hosseini, 2019). Managing and predicting these induced stresses is vital to ensuring the structural integrity and longevity of welded components.

Artificial Neural Networks (ANN) are computational models inspired by the human brain's network of neurons. They are capable of recognizing complex patterns and modeling nonlinear relationships within data sets, which traditional statistical methods may not efficiently cap ture (Haykin, 1999). In engineering and materials science, ANN has been successfully applied for prediction, classification, and control purposes, including the prediction of welding-induced residual stress by learning from experimental or simulated data (Patil and Suryawanshi, 2020).

1.2 Statement of the Problem

Residual stresses resulting from TIG welding processes pose significant challenges in the fabrication of welded structures. These stresses can lead to detrimental effects such as dimensional distortion, reduced fatigue strength, stress corrosion cracking, and eventual structural failure (Sindo and Ho\sseini, 2019). Conventional techniques for measuring residual stresses, including X-ray diffraction and hole-drilling methods, are often time-consuming, expensive, and require specialized equipment (Withers and Bhadeshia, 2001). Therefore, there is a pressing need for developing predictive models that can estimate the magnitude of residual stresses efficiently, enabling better process control and reduction of weld defects.

1.3 Aims and Objectives

The aim of this project is to develop a predictive model for the actual maximum stress (specifically residual stress) in TIG weldment using Artificial Neural Network(ANN).

To achieve this aim, the following objectives will be pursued:

i. Conduct a review of recent relevant existing literature on the application of Artificial Neural Networks in predicting the mechanical properties in TIG welded joints.

ii. Identify necessary TIG welding process (input) parameters and their range of values from previous studies.

iii. generate a robust experimental matrix using a suitable design expert component.

iv. Conduct TIG welding experiments on mild steel coupons and record the actual maximum stress values in the experimental samples.

v. analyze experimental results using ANN and develop a predictive model

vi. Evaluate the performance and adequacy of the developed model.

1.4 Scope of the Study

This study is confined to the application of ANN for predicting residual stresses induced during the TIG welding process. The research involves experimental welding under controlled parameters, stress measurement, ANN model development, and Finite Element Method (FEM) based simulation for validation. The study focuses exclusively on TIG welding and does not cover other welding methods or alternative predictive modeling techniques (Patil and Suryawanshi, 2020).

The scope of this research revolves around predicting the actual maximum stress encountered during the TIG welding process using ANN. TIG welding, widely used for precision welding applications (especially in stainless steel, aluminum, and other non-ferrous materials), involves complex thermal and mechanical phenomena. These result in residual stresses, distortions, and sometimes failure in weld joints. Understanding and predicting stress behavior accurately is critical for improving the quality, safety, and performance of welded components.

Since direct measurement of stress during welding is challenging, costly, and sometimes inaccurate due to environmental and physical limitations, this study proposes the use of ANN — a data-driven, intelligent computational technique — to model and predict actual maximum stress based on input parameters.

1.5 Significance of the Study

The significance of this study lies in its potential to enhance the understanding and control of residual stresses induced during TIG welding, a critical factor affecting weld quality and structural performance. By developing an ANN based predictive model, the study offers a cost-effective and efficient tool for anticipating stress levels

without the need for extensive experimental measurements, thereby reducing both time and resources in the welding industry (Patil and Suryawanshi, 2020).

Furthermore, an accurate prediction of residual stresses allows engineers to optimize welding parameters proactively, mitigating common weld defects such as cracking and distortion. This leads to improved safety, durability, and service life of welded components, which is particularly important in sectors such as aerospace, automotive, and construction where structural reliability is paramount (Sindo and Hosseini, 2019).

Finally, the integration of ANN with FEM simulation provides a robust framework for welding process optimization, combining empirical data and numerical analysis to achieve a deeper insight into the thermal and mechanical behavior of welded joints. This contributes to advancing welding technology and supporting ongoing research and development in materials engineering.

CHAPTER TWO

LITERATURE REVIEW

2.1 Welding

Welding is a fabrication process that involves the joining of two or more metal parts by applying heat, pressure, or both, to fuse them together permanently. It is widely used in industries such as automotive, construction, aerospace, and shipbuilding. Welding ensures strong and leak-proof joints that can sustain high mechanical loads and temperature conditions (Sindo and Hosseini, 2019).

It is the process of joining similar or dissimilar materials by the application of heat and/or pressure, with or without the addition of filler metal. Welding is a fabrication process that joins two or more materials, usually metals or thermoplastics, by applying heat, pressure, or both, causing fusion at the interface of the materials. Upon cooling, a metallurgical bond is formed that is typically as strong as or stronger than the base materials.-*American Welding Society (AWS), 2020*

2.1.1 Types of welding:

Welding processes can be broadly categorized into the following types

i. Arc Welding – Uses an electric arc to melt metals at the welding point. Examples include: Shielded Metal Arc Welding (SMAW), Gas Metal Arc Welding (GMAW or MIG) and Gas Tungsten Arc Welding (GTAW or TIG).

ii. Gas Welding – Uses a flame produced by burning gas (usually ox-acetylene) to melt the work pieces.

iii. Resistance Welding – Generates heat by passing current through the metal interface. Examples include spot welding and seam welding.

iv. Solid-State Welding – Includes processes such as friction welding and ultrasonic welding, where fusion is achieved without melting the base material.

v. Laser and Electron Beam Welding – High-precision processes used in advanced manufacturing sectors.

2.2 TIG Welding (Gas Tungsten Arc Welding)

TIG Welding or Gas Tungsten Arc Welding (GTAW), uses a non-consumable tungsten electrode to produce the weld. The weld area is protected from atmospheric contamination by an inert gas, typically argon or helium. A filler metal may or may not be used, depending on the application. American Welding Society. (n.d.). *Gas Tungsten Arc Welding (GTAW)*.

A TIG welding torch assembles several key components. A tungsten electrode is held by a collet in the torch head, while ceramic gas cups (pink) fit over the tip to direct the inert shielding gas onto the weld area. The inert gas (typically argon or a helium/argon mix) envelops the arc and molten pool, preventing oxidation. The welder manually controls the torch to form an arc with the workpiece; the electrode produces a small, focused arc that delivers intense heat exactly where needed. When filler metal is required, the operator adds a separate filler rod to the puddle. In practice, TIG welding uses a constant-current power supply (either DC or AC) to maintain a stable arc.

In DC polarity, the tungsten is normally connected to the negative output (DCEN) so that most heat is concentrated on the workpiece and the electrode stays cool. For materials with stubborn oxide layers (e.g. aluminum or magnesium), AC current is

used: each half-cycle switches polarity, providing both welding and a mild “cathodic cleaning” action that removes surface oxides. This dual polarity makes TIG especially effective for aluminum alloys. The arc can be initiated by a momentary spark (high-frequency start) or by briefly touching the electrode to the workpiece and lifting it. The inert gas flow rate is adjusted to cover the weld zone; higher flow or pure argon is used for very reactive metals, while argon/hydrogen or argon/helium mixtures can be used to increase weld speed and heat (at the expense of higher gas cost or risk of hydrogen cracking).

2.2.1 Applications of TIG Welding

Tungsten Inert Gas (TIG) welding is a precision welding technique widely used in industries that demand high-quality and defect-free joints. It employs a non-consumable tungsten electrode and an inert gas shield (usually argon or helium) to protect the weld area from atmospheric contamination according to Messler (2004). TIG welding is used across many industries wherever high weld quality and precision are required. Key applications include:

i. Aerospace and motor-sports: According to Cary and Helzer (2005), TIG is common in aircraft and space vehicle construction, as well as high-performance automotive and motorcycle fabrication. Its very precise arc and clean, defect-free welds make it ideal for critical structural joints in aluminum, titanium, stainless steels, and other alloys.
ii. Chemical, oil and gas, and power plants: TIG is extensively used for welding pipes, pressure vessels and boilers. In particular, orbital TIG systems (robotic or mechanized) weld pipe in chemical plants or nuclear plants without human intervention. For example, TIG welding is employed to seal spent nuclear-fuel

canisters because the welds match the base metal chemistry exactly and resist corrosion.

iii. Industrial fabrication: The process is widely used to weld thin sheets and tubing of stainless steel, aluminum, and other non-ferrous metals. It's routinely used for bicycle frames and thin-walled metal structures, as well as precision instrumentation and valve components.

iv. Maintenance, repair, and specialized equipment: TIG is often used for repair welding of dies, molds, and tools (especially aluminum and magnesium parts) because of its fine control and low heat input. It is also used in the food, beverage and pharmaceutical industries to weld sanitary stainless steel piping (yielding smooth, hygienic welds), and in art or architecture for decorative metalwork.

2.2.2 Advantages of TIG Welding:

TIG welding is often the process of choice when precision, control, and high-quality welds are critical. Its ability to produce clean, aesthetically pleasing, and defect-free joints offers numerous benefits in both structural and decorative applications. The following are key advantages that make TIG welding a preferred method in many industries:

i. Produces clean, high-quality, and precise welds.

ii. Suitable for thin materials and non-ferrous metals

iii. Minimal spatter and post-weld cleanup required.

iv. Excellent control over the welding arc.

2.2.3 Disadvantages of TIG Welding:

Despite its many strengths, TIG welding is not without limitations. Certain factors—such as operational complexity, cost, and time—can reduce its practicality in specific scenarios. Understanding these disadvantages is important for selecting the most efficient and cost-effective welding technique for a given application:

i. Slower process compared to other arc welding methods.

ii. Requires higher skill levels and training.

iii. Less suitable for thicker materials.

iv. Higher initial equipment cost.

2.3 The Identification of the Key Welding Process Parameters that Influence Residual Stresses in Tungsten Inert Gas

This chapter is the literature on parameters that influence residual stresses in tungsten inert gas welding. Residual stresses induced during TIG welding significantly affect the performance, reliability, and durability of welded structures. These stresses, which can be tensile or compressive, arise from the thermomechanical cycles experienced during welding, including rapid heating, melting, and cooling. According to a comprehensive review by Springer (2025), residual stresses in carbon steel weldments can lead to brittle fracture, fatigue failure, and stress corrosion cracking, particularly in the HAZ. The HAZ undergoes metallurgical transformations, such as the formation of martensite, which reduces ductility and toughness, increasing the risk of crack initiation under service loads.

Residual stresses are locked-in stresses that remain after welding due to uneven heating and cooling. In TIG (GTAW) welding, several critical parameters greatly influence the magnitude and distribution of residual stresses within the weldment.

i. Welding Speed (Travel Speed)

Heat input per unit length is inversely proportional to welding speed. Increased speed reduces the heat affected zone (HAZ), leading to quicker cooling and higher thermal gradients, which generally increase tensile stresses and localised distortion (Kutelu, *et al.* 2018). In their perspective, (Khan, *et al.* 2019) found welding speed to be the most dominant factor controlling longitudinal and transverse residual stresses in pulsed TIG applied to Ti-5Al-2.5Sn.

ii. Arc Current and Heat Input

Higher current increases arc power and deeper weld penetration, elevating peak temperatures and resulting in higher tensile stresses in the solidified weld (Minh, *et al.* 2024). A numerical model for stainless steel TIG welding indicated arc current is the most significant influence on compressive residual stress, followed by voltage and welding speed. Interaction effects: Elevated current combined with slower travel speed drastically raises residual stress levels (*Scientific. Net,* 2015).

iii. Arc Voltage

Voltage impacts arc length and heat input; it doesn't dominate as much as current or speed but still contributes to temperature fields. Notable interactions exist between voltage, current, and travel speed. Higher voltage can amplify stress effects when coupled with high current and low travel speed (Hu, *et al.* 2024).

iv. Pulse Parameters

Pulsed TIG adds variables: peak current, background current, pulse frequency/duty cycle. In pulsed TIG with Ti-alloys, peak current and welding speed were crucial in controlling residual stresses (Khan, *et al.* 2018).

v. Electrode-to-Work Distance (Arc Length)

Also known as stick-out or arc length. Longer arc increases heat spread and larger HAZ, affecting heat distribution and resulting stresses (Kutelu, *et al*, 2018).

vi. Shielding Gas Composition and Flow Rate

Gas type influences arc characteristics and thermal coupling: helium-rich mixtures increase heat input compared to argon (Marinelli, *et al.* 2019). The flow rate affects arc stability; too much causes turbulence (drawing in air), too little allows oxidation. Both can modify cooling rates and stress profiles (en wikipedia. org, 2010).

Welding speed is often the dominant lever controlling residual stress—especially when combined with current and heat input. Arc current and voltage significantly contribute to stress development, particularly when interlinked with travel speed. Pulse settings, arc length, and shielding gas composition fine-tune heat distribution and cooling rates, directly impacting stress profiles. Torch angle and tungsten health affect arc stability and consistency, influencing localized thermal stress. Using multi-pass welding, pulse TIG, and post-weld treatments can mitigate undesirable stress levels and distortion. Corroborating the aforementioned, (Khan, *et al.* 2019), in their study titled "Response surface approach to minimise the residual stresses in full penetration pulsed TIG weldments of Ti-5Al-2.5Sn alloy", demonstrated through experimental and statistical modelling that welding speed, peak current, and pulse parameters significantly affect residual stress profiles in TIG welding. They concluded that welding speed had the most dominant effect, while high peak current

and lower background current were also critical in controlling the thermal cycle and, consequently, the residual stress distribution. This study strongly supports the assertions made in the summary, particularly regarding the critical roles of welding speed, current, and pulse characteristics in determining residual stress magnitudes in TIG welding.

2.4 Residual Stress Formation:

Residual stress is the stress that remains in a material after the original cause of the stress such as mechanical loading, thermal gradients, or phase transformation has been removed. It is the non-uniform heating and cooling of the thermal expansion. These stresses can form during manufacturing processes like welding, casting, forging, machining, and heat treatment, According to Kou (2003).

Welding processes, including TIG, introduce residual stresses due to the localized heating and subsequent cooling cycles. These thermal cycles cause thermal expansion and contraction, leading to stresses that can result in distortions, cracks, or reduced structural integrity. (Barlam, *et al.* 2019), A study on "Residual stress analysis of dissimilar tungsten inert gas weldments of AISI 304 and Monel 400 by numerical simulation and experimentation" emphasizes that these stresses are critical, particularly in dissimilar welds, and can affect the service life of welded structures. The study used finite element modeling with ANSYS 16.0 to predict temperature fields and residual stress distribution, validating results experimentally using X-ray diffraction (XRD) technique, finding residual stresses within yield limits but highlighting the impact of uneven heating/cooling on thermal stresses near the fusion zone.

Mechanisms of Residual Stress Formation include:

i. Thermal Effects: During processes like welding or casting, non-uniform heating and cooling cause differential thermal expansion and contraction. If one part of a component cools and contracts faster than another, internal stresses develop to accommodate the deformation mismatch (Withers and Bhadeshia, 2001).

ii. Plastic Deformation: In processes like cold working or shot peening, plastic deformation at the surface while the bulk remains elastic leads to locked-in stresses. Compressive stress often remains on the surface while tensile stress is present in the interior.

iii. Phase Transformations: Changes in micro structure, such as the transformation of austenite to martensite in steels, are accompanied by volume changes. These volume mismatches can induce residual stresses (Totten and Howes, 1997).

iv. Mechanical Processing: Machining can introduce residual stresses due to the plastic deformation and localized heating near the cutting zone.

Types of Residual Stress

Residual stresses are often classified into three types:

i. Type I (Macro-stresses): Uniform over many grains, affecting large regions.

ii. Type II (Micro-stresses): Vary between different phases or grains.

iii. Type III (Micro-structural-level): Exist within individual grains due to defects like dislocations.

2.4.1 Effect Of Residual Stress on Welded Structures and Joints

Residual stresses significantly influence the performance, durability, and integrity of materials and structures. Their effects can be either beneficial or detrimental, depending on their nature (tensile or compressive), magnitude, and distribution. Below is an elaborated explanation of the effects of residual stresses with scholarly references According to (Howes, M. A. H. 1997). Residual stresses can have beneficial or detrimental effects. For example, Compressive surface residual stresses (from shot peening) can improve fatigue life.Tensile residual stresses (from welding) may lead to stress corrosion cracking or fatigue failure.Withers, P. J., and Bhadeshia, H. K. D. H. (2001). Totten, G. E., and Howes, M. A. H. (1997).

i. Mechanical Performance: This include, Fatigue Life which comprises of Tensile residual stresses reduce fatigue resistance by aiding crack initiation and propagation, Compressive residual stresses which comprises of induced by shot peering, retard crack initiation and are beneficial in fatigue-prone components, Compressive surface residual stresses delay the nucleation of fatigue cracks, thereby extending the fatigue life, whereas tensile surface residual stresses accelerate crack growth. (Withers and Bhadeshia, 2001).

ii. Stress Corrosion Cracking (SCC): This talks about Tensile residual stresses, especially at surfaces, can make materials susceptible to SCC, particularly in aggressive environments (e.g., chloride stress corrosion in stainless steels). It also talk about Residual tensile stresses are often a key contributor to stress corrosion cracking, particularly in welded or cold-worked components exposed to corrosive environments (Totten and Howe, 1997).

iii. Distortion and Dimensional Stability: Residual stresses can cause warping or distortion during or after manufacturing processes, such as machining, welding, or heat treatment. These dimensional instabilities can lead to tolerance issues in precision components. Even small residual stress gradients can cause significant distortion in thin or asymmetrical parts, leading to failure to meet dimensional tolerances (Liu and Alton, 2000).

iv. Fracture Behavior: Residual stresses can influence fracture toughness. Compressive stresses near a crack tip can reduce the driving force for crack propagation, increasing toughness. In contrast, tensile residual stresses near flaws or weld defects can lead to brittle fracture even under sub-critical loads. "Residual tensile stress fields can superimpose with external loads, significantly reducing the load-carrying capacity of cracked components"(Anderson, 2005)

v. Wear and Contact Fatigue: Compressive residual stresses in surface layers improve resistance to rolling contact fatigue and fretting wear. This is particularly exploited in the automotive and aerospace industries through surface treatments like carbonizing, nit-riding, and shot peering. Induced compressive stresses on gear surfaces are effective in improving wear resistance and increasing the load-carrying capacity"(Totten *et al.,* 2002).

vi. Manufacturing and Joining Processes: In welding, residual stresses can cause distortion or buckling of structure, can also lead to weld cracking or reduced fatigue life. Additive manufacturing (AM) processes are especially prone to high residual stresses due to rapid thermal cycling, which may necessitate post-process stress relief. Stress-relief annealing,Shot peering,Laser shock peering,Vibratory stress relief Pierson T. L. (2005), Schajer, G. S. (2010). Residual stresses in selective laser splintering and selective laser melting.

2.4.2 Types of Stress in Engineering Materials

In engineering, stress refers to the internal resistance offered by a material to an external force or load. It is a measure of the intensity of internal forces acting within a deformable body and is expressed in units of pressure (e.g., Pascals, Pa or N/m^2). Understanding the different types of stress is fundamental in assessing how materials and structures respond to various loading conditions. According to Beer *et al,* (2012), stress can be broadly categorised based on the direction and nature of the applied force. The most common types include tensile stress, compressive stress, shear stress, bending stress, and torsional stress.

i. Compressive Stress

Compressive stress occurs when forces act to shorten or compress a material. Like tensile stress, it is also defined by the ratio of force to area, but in the opposite direction. This is commonly found in columns, walls, and load-bearing foundations. If the stress exceeds the material's compressive strength, it may result in buckling or crushing. According to Hibbeler (2017), the failure of structures under compressive loads is often not due to the material strength itself but rather due to instability, particularly in slender members.

ii.Tensile Stress

Tensile stress arises when forces act to stretch or elongate a material. It is defined as the force applied perpendicular to the surface divided by the cross-sectional area. Tensile stress increases the length of a component and is common in structural elements such as cables, tie rods, and suspended bridges. If the stress exceeds the material's tensile strength, it may lead to ductile or brittle failure, depending on the material's properties (Callister and Rethwisch, 2020).

iii. Bending Stress

Bending stress (also called flexural stress) is a combination of tensile and compressive stresses that develop across a beam's cross-section when subjected to a bending moment. The fibres on one side of the neutral axis are stretched (tension), while those on the opposite side are compressed. Bending stresses are most relevant in beams, levers, and bridges, and they dictate design parameters such as section shape and support spacing (Beer *et al*., 2012).

iv. Shear Stress

Shear stress arises when forces are applied parallel or tangential to the surface of a material. It causes layers of the material to slide relative to one another. Shear stresses are critical in bolts, rivets, and beams under transverse loads. According to Megson (2014), materials subjected to shear are often designed to resist shear yield or rupture, which can be more sudden and less visible than tensile failure.

v. Torsional Stress

Torsional stress results from twisting actions applied to a component, causing shear stress over the cross-section. It occurs in shafts, axles, and other rotational elements. The stress distribution in torsion is circular, increasing with the radial distance from the centre. Torsional stresses are particularly important in power transmission systems and must be carefully managed to avoid twisting failures (Hibbeler, 2017).

2.4.3 Factors Influencing Residual Stress

Several factors influence the formation, magnitude, and distribution of residual stresses in materials. These factors are related to material properties, processing methods, and component geometry. Understanding these influences is essential to predict, control, or exploit residual stresses in engineering applications. They include:

i. Thermal Gradients: Residual stresses often arise due to non-uniform heating and cooling during manufacturing processes such as welding, casting, heat treatment, and additive manufacturing. Parts of a component expand and contract at different rates, creating internal stress fields once the part reaches a uniform temperature.

Thermal residual stresses result from differential expansion or contraction during heating and cooling cycles, especially when large temperature gradients exist within the material Withers and Bhadeshia (2001).

ii. Plastic Deformation and Work Hardening: Processes like machining, cold rolling, or shot peening cause surface plastic deformation while the underlying material remains elastic. When the external load is removed, a mismatch in elastic recovery induces residual stresses.Mechanical working induces plastic strain in surface layers, and the elastic mismatch with the underformed core leads to residual stress development. Totten et al. (2002).

iii. Phase Transformations: materials like steel, phase transformations (e.g., austenite to martensite) during cooling involve volume changes. These transformations can generate significant internal stresses. Phase transformations that involve volumetric changes, such as the martensitic transformation, are a major source of residual stress in heat-treated steels. Bhadeshia (1999).

iv. Material Properties: intrinsic material properties influence how stresses develop and are retained Thermal conductivity: Influences the speed of heat dissipation.Thermal expansion coefficient: Affects how much a material expands/contracts with temperature.Elastic modulus and yield strength: Define how easily a material can deform elastically or plastically.Materials with low thermal conductivity tend to accumulate high thermal gradients, while those with low yield

strength accommodate stress by plastic deformation, reducing residual stress retention. Mercelis and Kruth (2006)

v. Manufacturing Process Parameters: Specific parameters like cooling rate (fast vs. slow),Tool feed rate and cutting speed,Welding speed and heat input,Layer thickness in additive manufacturing directly affect stress magnitudes and gradients.Prime (2001).

Residual Stress Relaxation Mechanisms: Even after formation, residual stresses can evolve due to Creep,Stress relaxation,Thermal exposure,Vibratory stress relief or annealing.

2.4.4 Measuring the Actual Maximum Stress in the Weldments Using Stress-Measurement Techniques.

This focuses on measuring the actual maximum stress in the weldments using stress measurement techniques in alignment with the aim / objective of the study. As it was earlier defined, welding is a process that joins materials by heating them to a molten state and allowing them to solidify into a cohesive joint, often with the addition of a filler material. TIG welding, or GTAW, is a high-precision method that uses a non-consumable tungsten electrode and an inert shielding gas to protect the weld area from contamination. It is widely used for its ability to produce high-quality, defect-free welds in thin materials and for applications requiring strict quality control, such as aerospace components and nuclear reactors (American Welding Society, 2020),Webster,(2002). The following are the methods used to measure actual maximum stresses in TIG-welded structures, with emphasis on widely-used residual stress techniques:

i. Semi-Destructive Mechanical Relaxation Techniques

a.) Hole-Drilling Method: The hole-drilling technique, as specified in ASTM E837, is a semi-destructive method for assessing near-surface residual stresses. A strain-gauge rosette is fixed to the surface, and a small blind hole is drilled at its centre. The relieved strains are measured and converted into biaxial stresses using calibration constants derived from theory and finite-element modelling. It is portable, suited to on-site work, and provides reliable results for shallow depths (about 1 mm or up to roughly the hole diameter). However, it does not capture deep stresses, slightly damages the surface, and accuracy depends heavily on rosette installation, drilling precision, and calibration quality.

b.) Deep-Hole Drilling (DHD): The deep-hole drilling (DHD) method is a semi-invasive technique for measuring residual stresses through the full thickness of a component. A fine reference bore is drilled, its diameter measured, and then a concentric core is trepanned to release stresses; the bore diameter is re-measured, and the difference is used to reconstruct the stress profile. It provides detailed through-thickness, often multi-axial, stress information with minimal effect on the component's integrity, making it highly valuable for thick metallic or composite parts. It is accurate and adaptable to various materials, but it requires specialised equipment, precise preparation, and is not practical for thin sections.

ii. Destructive Sectioning Techniques

Contour Method

Process: Cuts the specimen, measures surface deformation of the cut face, then reconstructs original stress field. It captures a full 2D stress map on a cut plane. Requires wire-EDM and precise deformation scanning.

Slitting and Sachs' Boring

Slitting: Cuts a slit and measures strain relief along length—useful for through-thickness stress profiles.

Sachs' Boring: Drills core and measures deformation—similar to hole drilling but more invasive.

iv. Non-destructive Diffractive Techniques

Neutron Diffraction

Principle: Measures interatomic spacing changes in bulk materials using high-penetration neutrons—enabling through-thickness residual stress mapping.

Example: Applied Physics A (2002) used neutron diffraction on an aluminium TIG weld (172×150×3 mm plate), revealing tensile longitudinal stress up to ~200 MPa in the weld, decreasing towards edges. Their 2×2×2 mm^3 gauge validated well against FE models . The advantages are: deep penetration (cm-level), true 3D strain mapping, non-destructive. The limitations, are: requires neutron facilities, time-consuming and complex data calibration (d_0 reference).

X-Ray Diffraction (XRD)

Principle: Measures elastic lattice strains via shift in diffraction peaks; limited to surface and near-surface layers (tens of μm). Example: Parikin *et al* (2017) measured residual stress on TIG welds in 57Fe-15Cr-25Ni steel using XRD for surface stress mapping. The limitations, are: limited penetration depth, sensitive to surface roughness and texture, complement with Neutron Diffraction.

A hybrid approach: XRD for surface profiling and neutron diffraction for bulk distribution, as shown in Harati *et al.*'s steel weld experiments.

2.4.5 Measuring Actual Maximum Stress in TIG Weldments

Methodology Overview

i. Identify relevant plane and location, typically near weld toe or HAZ.

ii. Select appropriate technique based on desired resolution, depth, and sample access.

iii. Calibrate instrument (d_0 reference for XRD/neutron, FE calibration for hole drilling).

iv. Measure residual strain or deformation.

v. Convert measured values to stress via Bragg's law (diffraction) or elasticity theory (hole drilling).

vi. Assess uncertainties and interpret peaks (σ_max).

Below, are examples of aluminium and steel TIG Weld:

Neutron diffraction scan across a bead-on-plate TIG weld using 2×2×2 mm^3 gauge volumes mapped longitudinal stress up to ~200 MPa .

Example: Steel TIG Girth Welds:

Neutron diffraction on S355G14+N pipe girth welds (multi-pass TIG) using POLDI diffractometer, mapping axial, hoop, and radial stress at depths 2–6 mm with ~3.8 mm gauge volumes. Hybrid study on S235 steel TIG welds reported maximum subsurface stresses through diffraction and stray field correlation (Mishurova *et al,* 2022).

Scientific Consensus on Maximum Stress Measurement

i. Neutron diffraction is consistently validated as accurate and deep-penetrating—for aluminium, steel, titanium weld.
ii. Combined diffraction (neutron + XRD) is especially valuable at capturing steep near-surface gradients.
iii. Hole and deep-hole drilling offer reliable near-surface and through-thickness mapping with portable equipment.

iv. Destructive techniques like contour method enable planar stress mapping but require sacrificing samples.

Recommended Workflow for Maximum Stress Determination

i. Preliminary mapping: Use neutron diffraction to identify bulk stress peaks (≈mm resolution).
ii. Surface profiling: Apply XRD to detect extreme stress concentrations near the weld toe.
iii. 3. Localized probing: Use hole drilling to confirm resolution at precise locations.
iv. 4. Deep insight: Apply deep-hole drilling in critical structural zones (e.g. pipe girth welds).
v. 5. Validation: Correlate with destructive techniques or stray-field analysis where accessible.

2.5 Optimisation and Prediction of Welding Process Parameters

Welding is a complex manufacturing process that involves multiple variables, including voltage, current, welding speed, shielding gas, and electrode type. The quality of the weld is highly dependent on the careful selection and control of these process parameters. As such, the optimisation and prediction of welding parameters play a critical role in ensuring consistency, quality, efficiency, and cost-effectiveness in industrial fabrication.

2.5.1 Importance of Welding Process Parameters

Welding parameters have a significant effect on weld bead geometry, mechanical properties, heat-affected zone (HAZ), residual stresses, and defects such as porosity and cracking. If parameters are not appropriately selected, the weld quality may

deteriorate, leading to structural failures. According to Kou (2003), minor changes in process parameters can lead to dramatic variations in metallurgical properties, particularly in fusion welding processes like GTAW and GMAW.

Optimisation Techniques

i. Taguchi Method

The Taguchi method is a statistical tool that reduces variability and improves quality through design of experiments (DOE). It uses orthogonal arrays to determine the most influential parameters with minimal experiments. Researchers have used this method to optimise TIG welding parameters like current, gas flow rate, and electrode gap to achieve desired penetration and tensile strength (Palani and Murugan, 2006).

ii. Response Surface Methodology (RSM)

RSM is a mathematical and statistical technique for modelling and analysing the influence of several variables on response variables. It allows researchers to build predictive equations and locate optimal welding conditions. RSM has been widely applied in MIG, TIG, and laser welding to control bead geometry and minimise distortion (Kannan *et al.* 2018).

iii. Genetic Algorithms (GA)

Genetic algorithms simulate natural selection processes to find optimal welding parameters. GA is effective in multi-objective optimisation where trade-offs between parameters like tensile strength and heat input must be balanced. According to Deb (2001), GA offers a robust approach to global optimisation, especially when dealing with non-linear and multi-modal surfaces.

2.5.2 Prediction Techniques

i. Artificial Neural Networks (ANN)

ANNs are machine learning models that mimic human brain function. They are widely used for predicting welding outcomes such as tensile strength, bead width, and hardness based on input parameters. Studies have shown that ANN models trained on experimental data can accurately predict weld quality and help reduce costly trial-and-error procedures (Kumar and Sundarrajan, 2009).

ii. Regression Models

Multiple linear regression (MLR) and non-linear regression models are commonly used for welding parameter prediction. These models can quantify the relationship between input variables (current, speed, etc.) and output (hardness, porosity). While they may not capture complex patterns like ANNs, they offer interpretability and simplicity (Montgomery, 2017).

iii. Support Vector Machines (SVM) and Random Forests

More advanced machine learning algorithms like SVM and Random Forests have also been implemented in welding process modelling. They provide high prediction accuracy and can handle non-linear, high-dimensional data efficiently (Zhao, Liu and 2019).

iv. Finite Element Method (FEM)

The Finite Element Method (FEM) is a numerical technique widely used for solving complex engineering and physical problems involving stress analysis, heat transfer, fluid dynamics, and electromagnetic fields. It is based on dividing a large, complex system into smaller, simpler parts called finite elements, which are then analysed individually and assembled to form a complete solution (Logan, 2016).

Industrial Applications

Industries such as automotive, aerospace, shipbuilding, and oil and gas routinely use optimised welding parameters to meet stringent quality standards. Automated robotic welding systems often incorporate real-time monitoring and predictive algorithms to adjust process parameters on the fly, improving efficiency and reducing defects (Ravichandran and Arivazhagan, 2015).

2.5.3 Benefits and Limitations

Benefits

i. Enhanced weld quality and consistency
ii. Reduction in defects and rework
iii. Lower material and energy consumption
iv. Better process control and automation
v. Informed decision-making through predictive modelling

Limitations

i. Requires high-quality experimental data for model training
ii. Computational cost for advanced algorithms
iii. May not generalise well outside trained conditions
iv. complex optimisation techniques can be difficult to implement without expert knowledge

2.6 Artificial Neural Network (ANN)

ANN are a class of machine learning algorithms inspired by the structure and function of biological neural networks. They consist of interconnected groups of artificial neurons organized in layers (input, hidden, output) that process information using a

connectionist approach to computation.H *aykin, S. (2009). Neural Networks and Learning Machines (3rd ed.). Pearson.*

It is is a computational model inspired by the structure and functioning of the human brain. It consists of interconnected processing elements called neurons, organized in layers, that work together to solve specific problems such as pattern recognition, prediction, or classification by learning from data. Zhang, *et al.* (2017).

It is important as it is capable of learning non-linear relationships, easily adaptable to complex and noisy data,suitable for multi variable optimization, as it also enables real-time prediction and control when integrated with sensors.

ANN offers a promising alternative because they can learn arbitrary non-linear mappings from welding inputs to stress outcomes. ANN have been applied to welding problems and shown to produce stress predictions highly, efficiently, and greatly reducing the time required compared to full simulations. By training on data (from experiments or simulations), an ANN could rapidly estimate the peak stress in a TIG weld given the process parameters, without the need for on-the-fly finite element (FE) analysis. Welding engineering currently lacks accessible, real-time stress-prediction tools. Some specialized software (for example, the E-Weld Predictor tool) can compute weld stresses from user-provided parameters, but these generally rely on offline FE back-ends and do not operate during actual welding. Recent research suggests machine-learning methods could achieve near-real-time stress forecasts. This is a feat beyond conventional simulations, which according to Southwest Research Institute (2025), remain complex, time- consuming, and unable to run at a rate that could support production.

2.6.1. Structure of an ANN Used in Welding Applications

A basic ANN comprises:

i. Input Layer: Receives data in numerical form (features).

ii. Hidden Layer(s): One or more layers where neurons transform inputs using eights and activation functions.

iii. Output Layer: Produces the prediction or classification result.

Each connection between neurons has an associated weight. During training, these weights are adjusted using algorithms like back propagation to minimize the error between predicted and actual outputs.*Basak, S., and Majumder, A. (2014).*

2.6.2 Benefits of ANN in Welding

In engineering, ANN are used for:

i. Predicting mechanical properties of materials (e.g., tensile strength, fatigue life.

ii. Automation: Easily integrated into intelligent systems for real-time weld control.

iii. Weld quality prediction and optimization.

iv. Structural health monitoring.

v. Adaptability: Can be trained for various welding processes (e.g., TIG, MIG, laser).

How Ann Carries Out Prediction

An Artificial Neural Network (ANN) carries out prediction by learning patterns and relationships from input data during a training phase, and then using those learned weights and biases to predict outputs for new, unseen data. It comprises of Input Layer which involves feeding the data, Forward Propagation that talks about how

the data is being transformed to introduce non-linearity.(e.g., ReLU, sigmoid). The error is minimized using back propagation and optimization algorithms like Stochastic Gradient Descent (SGD) or Adam.(Dally, J. W., and Riley, W. F.1991).

In Prediction Phase, it uses trained model and ANN to input new input and he model uses the stored weights and biases to compute outputs. Also, no further learning happens during this stage.

Input Layer Receives features (e.g., TIG welding parameters)

Hidden Layers Process inputs using weights, bias,activation

Output Layer Generates prediction (e.g., stress, defect class).Haykin, S. (2009)

2.6.3 Application Of ANN Welding

ANN have become a valuable tool in welding technology, offering data-driven solutions to complex problems that are difficult to solve using traditional analytical methods. Kim, I. S., Basu, A., and Jung, Y. S. (2005).

In TIG welding, ANNs are often used to:

i. Predict mechanical properties (e.g., tensile strength, hardness, residual stress).
ii. Identify or classify welding defects (e.g., porosity, cracks).
iii. Optimize process parameters (e.g., gas flow rate, electrode type).

A trained ANN can predict the maximum tensile stress in a TIG-welded joint based on input parameters like current, voltage, welding speed, and material thickness. Haykin, S. (2009). *Neural Networks and Learning Machines* (3rd ed.).

It is used in predicting residual stress,estimating weld bead geometry,classifying defect types and for controlling welding parameters in real time. Chen, J., *et al.* (2017).

2.6.4 Training and Validation of ANN Models

To ensure high prediction accuracy, ANN models must be trained using a large, diverse, and high-quality data set. The training involves:

i. Forward propagation (initial prediction)
ii. Back propagation (error correction)
iii. Weight adjustment (learning)

2.7 Limitations of the Study

The study has several limitations that define its scope:

i. Assumptions in Surrogate Modeling: The ANN may not capture all physical complexities of the welding process, such as arc behavior, material variability, or environmental factors, which are better modeled by FEA.
ii. Dependence on Training Data: The accuracy of the ANN model depends heavily on the quality and quantity of training data, which may be limited by the availability of FEA simulations or experimental measurements.
iii. Specific Materials and Configurations: The study is limited to certain materials (e.g., stainless steel, aluminum) and joint types (e.g., butt, fillet), as opposed to a comprehensive analysis across all possible materials and geometries.
iv. No Real-Time Control: The scope does not include implementing the ANN model in real-time welding systems for adaptive control; it focuses on prediction and optimization based on simulated data.

v. Simulation-Based Approach: The focus is on ANN-based surrogate modeling, not on conducting physical welding experiments for data collection. While validation may involve experimental data, the primary dataset for training comes from simulations.

2.8 Safety Procedures During Welding

Welding involves high temperatures, electric currents, radiation, fumes, and flammable materials, making it a potentially hazardous process. To prevent accidents and health issues, the following proper safety procedures is essential:

i. Electrical Safety: Inspect welding cables and electrode holders for damage before use, to ensure equipment is properly grounded.cal parts.Turn off the power source when not welding or changing electrodes.

ii. Fire and Explosion Prevention- Use welding screens to contain sparks.

iii. Ventilation and Fume Control - Use local exhaust ventilation (LEV) or fume extraction systems to remove fumes at the source.Work in a well-ventilated area, especially when welding metals like stainless steel, galvanized steel.

iv. UV/IR Radiation Protection - Welding arcs emit intense ultraviolet (UV) and infrared (IR) radiation, which can cause eye injuries ("arc eye") and skin burns.Use a properly shaded welding helmet (typically shade #10–13).Ensure bystanders are protected using welding curtains or screens.

v. Safe Work Environment- Maintain a clean, organized workspace to prevent tripping hazards.Use non-slip surfaces where possible.Never weld near water unless special precautions are taken.

vi. Training and Certification- Only trained and qualified personnel should perform welding.Understand the Material Safety Data Sheets (MSDS) for materials being welded.Follow standard procedures and codes (e.g., OSHA, AWS, ISO).

vii. First Aid and Emergency Preparedness.Know the location of first aid kits, emergency exits, and eye wash stations.Be trained in basic first aid for burns, electrical shock, and eye injuries.

2.8.1 Common Hazards in Welding

Welding hazards can be grouped into the following categories (Jeffus, 2012; HSE, 2018):

i. Radiation Exposure: Ultraviolet (UV) and infrared (IR) rays from the welding arc can cause “arc eye” or retinal burns.
ii. Toxic Fumes and Gases: Inhalation of fumes (e.g., zinc, manganese, chromium) and shielding gases can cause respiratory diseases.
iii. Electric Shock: A major cause of injury or fatality in arc welding if proper grounding and insulation are not used.
iv. Fire and Explosions: Sparks and spatter can ignite flammable materials in the environment.
v. Burns: Contact with molten metal or hot surfaces causes severe thermal injuries.
vi. Noise Exposure: High noise levels from welding equipment can lead to hearing loss over time.
vii. Mechanical Hazards: Injuries from heavy machinery or poor handling of work pieces.

2.8.2 General Safety Procedures

Personal Protective Equipment (PPE) refers to specialized clothing or gear worn by workers to protect themselves from hazards that can cause injury or illness in the workplace. PPE acts as a barrier between the wearer and potential dangers such as physical, chemical, biological, electrical, or radio logical risks. They include:

i. Hard hats or helmets protect your head from falling objects or impacts.

ii. Safety goggles or glasses shield your eyes from dust, flying debris, chemicals, or harmful radiation.

iii. Face shields protect your entire face from splashes, sparks, or intense light (commonly used in welding).Earplugs and earmuffs reduce exposure to loud noises that can damage hearing.

iv. Respirators or dust masks help filter out harmful dust, fumes, or gases you might breathe in.

v. Gloves protect your hands from cuts, burns, chemicals, or electrical hazards. Examples include leather gloves for welding or nitrile gloves for handling chemicals.

vi. Steel-toed boots or safety shoes protect your feet from heavy falling objects, punctures, or electrical hazards.

vii. Flame-resistant clothing or coveralls protect your body from heat, sparks, or flames.

viii. Safety harnesses and lanyards are used to prevent falls when working at heights.

CHAPTER THREE

METHODOLOGY

In the previous chapter we made a perspective sketch of the various relevant research works surrounding the present research study. In this chapter we shall explain the research strategy to be employed to obtain and analyze data for the study. The methodological steps are as follows;

i. Identification of input parameters range

ii. Samples and sampling technique

iii. Experimental data collection

iv. Experimental data analysis

3.1 Identification of Input Parameters Range.

The key parameters to be considered in this work are welding current (A), welding voltage (V), Gas Flow Rate (L/Min). The range of the process parameters to be used were gotten from relevant recent literature is tabulated below.

Table 3.1: Process parameters and their levels

PARAMETERS	UNITS	SYMBOL	MINIMUM VALUE	MAXIMUM VALUE
Welding Current	Amps	I	160.00	190.00
Welding Voltage	Volts	V	22.00	25.00
Gas Flow Rate	L/Min	GFR	14.00	17.00

.Erhunmwunse B.O and Ozigagun A. (2021).

The following materials and equipment would be used to effectively and successfully carry out this research study: mild steel plates, power hacksaw, a TIG welding machine, argon gas and a universal stress testing machine.

3.2 Samples and sampling technique

The weld samples will be made from mild steel plates and cut to size using hack saw, edges grinded, surface polished with emery paper and the joint welded. A tungsten inert gas welding equipment will be used to carry out the welding process on the mild steel plates. The TIG welding process will use a shielding gas to protect the weld specimen from atmospheric interaction, 100% pure Argon gas will be used for this research study. The TIG welding machine alongside the argon gas is as shown in

Fig 3.1: TIG welding machine and equipment

Fig 3.2: Argon gas cylinder

Universal Stress Testing Machine

A Universal Stress Testing Machine (commonly known as a Universal Testing Machine, or UTM) is a multi-purpose material testing instrument used to evaluate the mechanical properties of materials under various types of loading conditions, such as tension, compression, bending, and shear. It is termed “universal” because it can perform a wide range of standardised mechanical tests on diverse materials including metals, plastics, ceramics, polymers, and composites (Budynas and Nisbett, 2015).

Fig 3.3: Universal stress testing machine

3.3 Experimental Data Collection

The input parameters (Current, Voltage and Gas flow rate) will be used as factors for the design matrix. The central composite design (CCD) interphase of VERSION 13.05 Design Expert will be used to developed a statistical design of experiment. The CCD matrix utilizing the three input parameter generated an experimental design matrix having six (6) center points (n_o), six (6) axial points (2n) and eight (8) factorial points (2^n) which when imputed into Equation 3.1 resulted in twenty (20) experimental runs. The CCD matrix is presented in Table 3.2. The total number of experimental runs as generated by the CCD is given as:

$$N = 2^n + n_o + 2n \quad (3.1)$$

where;

N: is the number of experimental runs based on CCD, 2^n: is the number of factorial points, n_o: is the number of center points, 2n: is the number of axial points and n: is the number of variables. Table 3.2 shows the experimental matrix generated by the CCD.

Table 3.2 Central Composite Design (CCD) Experimental Matrix Factors

Run	Factor 1	Factor 2	Factor 3
	A: Current (Amp)	B: Voltage (Volt)	C: Gas Flow Rate (lit/min)
1	170	22	14
2	170	23	15
3	190	24	16
4	170	25	17
5	180	22	15
6	170	23	16
7	180	24	17
8	160	25	14
9	180	22	16
10	160	23	17
11	160	24	14
12	160	25	15
13	180	22	17
14	170	23	14
15	170	24	15
16	170	25	16
17	170	25	17
18	170	24	14
19	160	23	15
20	170	22	16

CHAPTER 4

RESULTS AND DISCUSSION

4.1 Results

In this study, twenty (20) experimental runs were carried out, each experimental run comprising the current, voltage and gas flow rate. For each experimental run, the actual maximum stress was measured. The result presented in table 4.1

Table 4.1: Experimental result

Run	**PROCESS FACTORS**			
	1	2	3	RESPONSE
	A: Current	B: Voltage	C: Gas Flow Rate	Actual Max Stress
	(Amp)	(Volt)	(lit/min)	(MPa)
1	170	22	14	356.04
2	170	23	15	356.08
3	190	24	16	312.17
4	170	25	17	317.74
5	180	22	15	355.39
6	170	23	16	356.80
7	180	24	17	314.32
8	160	25	14	355.71
9	180	22	16	355.39
10	160	23	17	356.60
11	160	24	14	348.34
12	160	25	15	355.71
13	180	22	17	355.39
14	170	23	14	356.80
15	170	24	15	344.07
16	170	25	16	317.74
17	170	25	17	317.74
18	170	24	14	344.07
19	160	23	15	356.60
20	170	22	16	356.04

4.1.1 Prediction Using Artificial Neural Network (ANN)

Twenty (20) experimental data generated by replicating the design matrix from the CCD was used for the neural network modelling. The input and output data training resulting in the design of the network architecture is paramount in the application of neural network to data modelling and prediction. To obtain the optimal network architecture that possesses the most accurate understanding of the input and output data, two factors were considered. First was the selection of the most accurate training algorithm or learning rule and secondly, the number of hidden neurons. Based on these considerations, different training algorithm and hidden neurons were selected and tested to determine the best training algorithm and the optimum number of hidden neurons that will produce the most accurate network architecture.

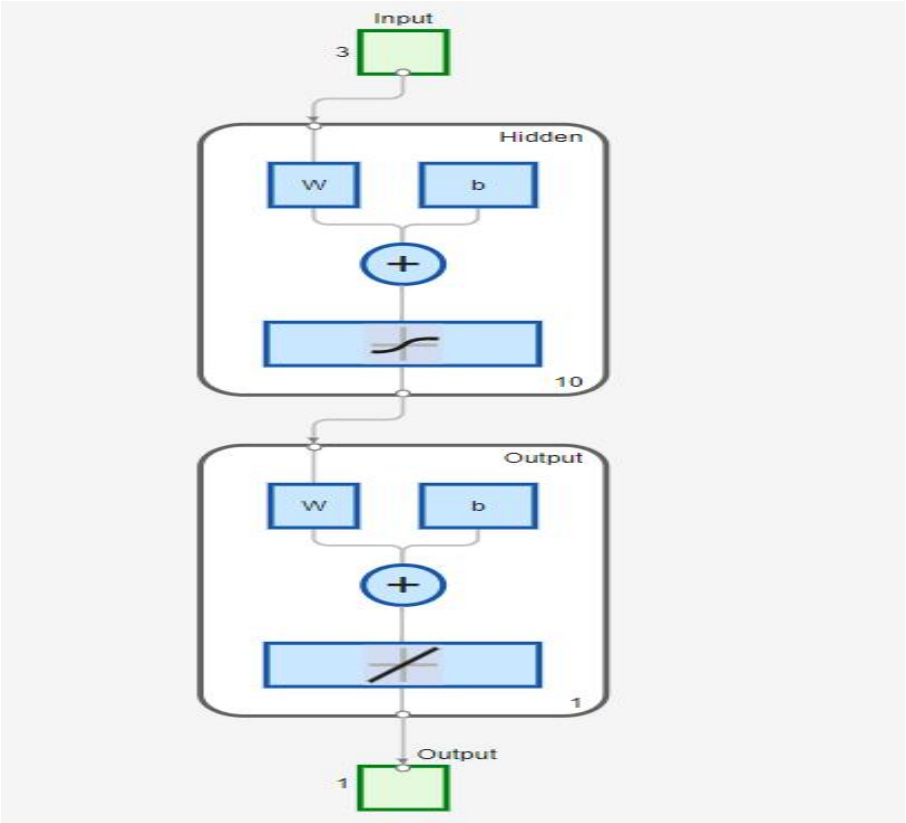

Figure 4.1: Artificial neural network architecture

The Artificial Neural Network architecture is 3-10-1, the network diagram generated for the prediction of actual maximum stress using the back propagation neural network is presented in Figure 4.1

Model Summary

Train a neural network to map predictors to continuous responses.

Data

Predictors: Input - [3x20 double]

Responses: Resp - [1x20 double]

Input: double array of 20 observations with 3 features.

Resp: double array of 20 observations with 1 features.

Algorithm

Data division: Random

Training algorithm: Levenberg-Marquardt

Performance: Mean squared error

Training Results

Training start time: 23-Oct-2025 20:23:27

Layer size: 10

	Observations	MSE	R
Training	14	0.3749	0.9993
Validation	3	80.6689	0.9279
Test	3	34.0843	0.9440

Fig 4.2 Model Summary for Predicting Actual Maximum Stress

ANN to train the neural network to mark prediction for continuous response the data was set for prediction and response. Input was set for twenty (20) observations which are current, voltage and gas flow rate while the response was set for twenty (20) observation which is the actual maximum stress. The training algorithm had a random data division using the levenberg Marquardt training algorithm using mean square error (MSE) as performance determinant. From the twenty (20) observations 14 was

used for training with MSE of 0.3479 and R value of 0.9993 while 3 was used for validation having a MSE of 80.6689 and R value of 0.9279 and 3 was used for test having a MSE of 34.0843 and R value of 0.9440.

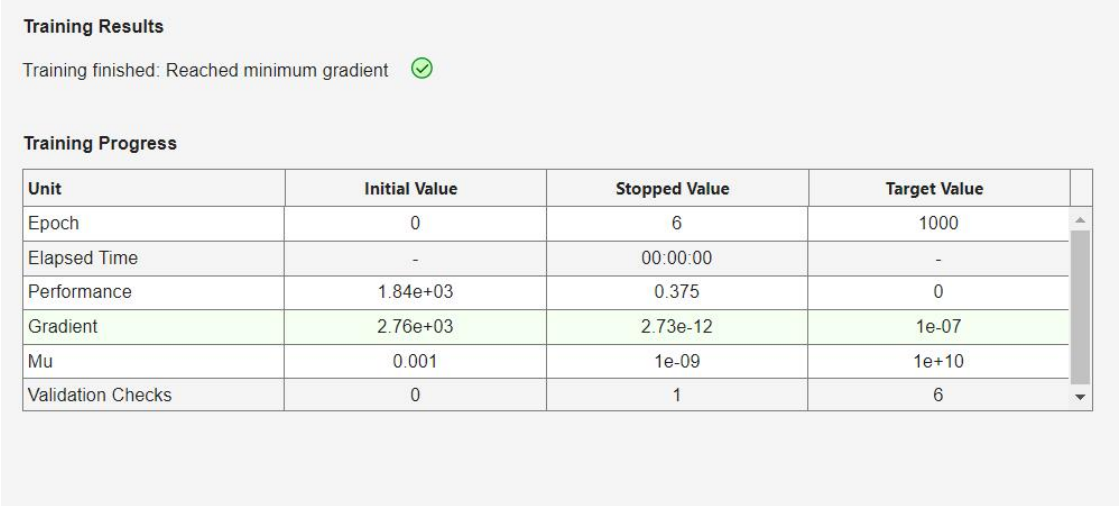

Training Results

Training finished: Reached minimum gradient

Training Progress

Unit	Initial Value	Stopped Value	Target Value
Epoch	0	6	1000
Elapsed Time	-	00:00:00	-
Performance	1.84e+03	0.375	0
Gradient	2.76e+03	2.73e-12	1e-07
Mu	0.001	1e-09	1e+10
Validation Checks	0	1	6

Figure 4.3: Training Results for Predicting Actual Maximum Stress

From the network training diagram of Figure 4.2, it was observed that the network performance was of 1.18e+03. Validation checks of one (1) was recorded out of six (6). However, this is expected since the issue of weight biased had been addressed via normalization of the raw data. A performance evaluation plot which shows the progress of training, validation and testing is presented in Figure 4.5

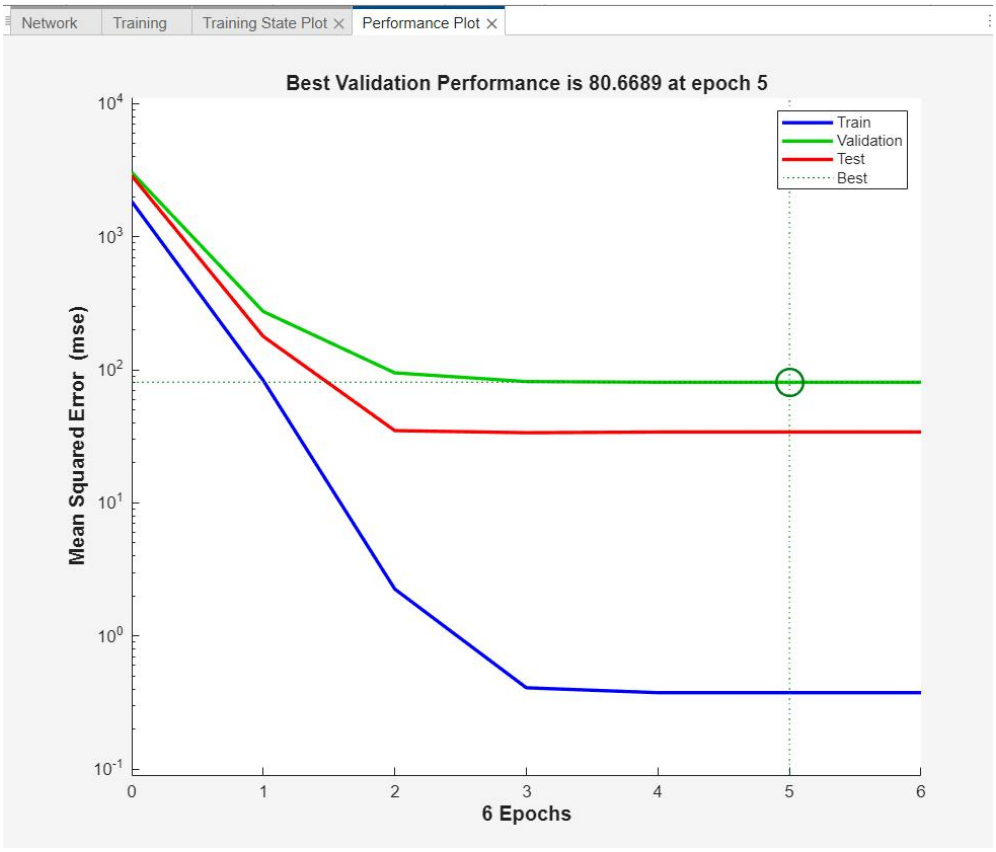

Figure 4.4: Performance Curve of Trained Network for Predicting Actual Maximum Stress

From the performance plot of Figure 4.3, no evidence of over fitting was observed. In addition, similar trend was observed in the behaviour of the training, validation and testing curve which is expected since the raw data were normalized before use. Lower mean square error is a fundamental criterion used to determine the training accuracy of a network. Best validation performance of 80.6689 at epoch 5 is evidence of a network with strong capacity to predict the actual maximum stress.

The training state, which shows the gradient function, the training gain (Mu) and the validation check, is presented in Figure 4.4

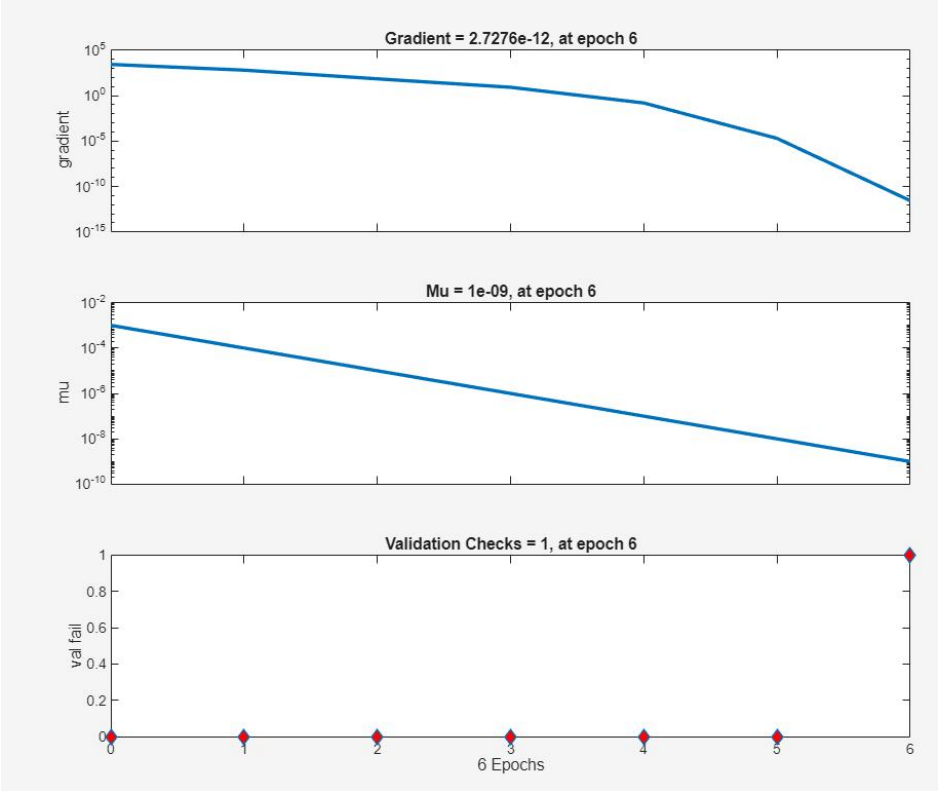

Figure 4.5: Neural Network Training State for Predicting Actual Maximum Stress

Back propagation is a method used in artificial neural networks to calculate the error contribution of each neuron after a batch of data training. Technically, the neural network calculates the gradient of the loss function to explain the error contributions of each of the selected neurons. Lower error is better. Computed gradient value of 2.7276e-12 as observed in Figure 4.4 indicates that the error contributions of each selected neurons is very minimal. Momentum gain (Mu) is the control parameter for the algorithm used to train the neural network. It is the training gains and its value must be less than unity. Momentum gains of 1e-09 shows a network with high capacity to predict the actual maximum stress. The regression plot which shows the correlation between the input variables (current, voltage and gas flow rate) and the target variable (maximum stress) coupled with the progress of training, validation and testing is presented in Figure 4.5.

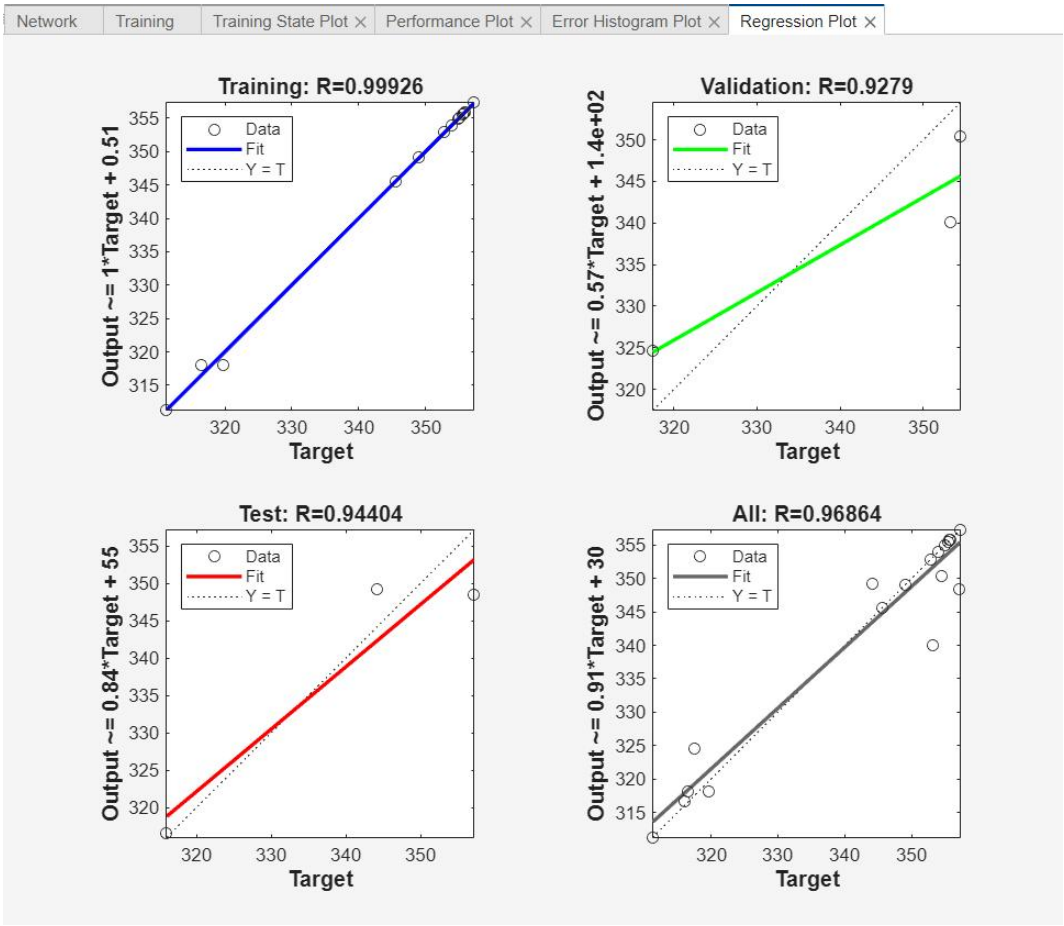

Figure 4.6 Regression Plot Showing the Progress of Training, Validation and Testing

Based on the computed values of the correlation coefficient (R) as observed in Figure 4.5, it was concluded that the network has been accurately trained and can be employed to predict the actual maximum stress. Figure 4.5 illustrates the regression plots for the training, validation, testing, and overall datasets of the developed Artificial Neural Network model. The plots compare the network outputs against the target values. The regression coefficient (R) values of training at 99.93%,validation at 92.79%, testing at 94.40% and overall data at 96.86% respectively indicate a strong correlation between the predicted and experimental values.

The ANN actual maximum stress considering the input parameters(current, voltage and gas flow rate) for 20 runs is as presented in table 4.2

Table 4.2: The ANN maximum stress result

Run	Current (A)	Voltage (V)	Gas Flow (l/min)	ANN Max Stress (MPa)
1	170	22	14	355.04
2	170	23	15	354.97
3	190	24	16	311.28
4	170	25	17	318.08
5	180	22	15	350.384
6	170	23	16	353.97
7	180	24	17	316.603
8	160	25	14	340.036
9	180	22	16	352.85
10	160	23	17	357.3
11	160	24	14	349.07
12	160	25	15	355.52
13	180	22	17	355.85
14	170	23	14	355.75
15	170	24	15	349.2
16	170	25	16	324.6
17	170	25	17	318.08
18	170	24	14	345.6
19	160	23	15	348.422
20	170	22	16	355.73

A comparison was then made with error margin between the experimental values and ANN predicted values as presented in table 4.3

Table 4.3: Experimental values vs ANN

Run	Current (A)	Voltage (V)	Gas Flow (l/min)	Experimental Max Stress (MPa)	ANN Max Stress (MPa)	Error
1	170	22	14	355.04	355.04	1.1301E-08
2	170	23	15	354.97	354.97	5.9815E-08
3	190	24	16	311.28	311.28	7.0391E-08
4	170	25	17	319.7	318.08	1.62
5	180	22	15	354.44	350.384	4.05590489
6	170	23	16	353.97	353.97	1.015E-07
7	180	24	17	316.02	316.603	-0.5830423
8	160	25	14	353.26	340.036	13.2236759
9	180	22	16	352.85	352.85	7.5905E-07
10	160	23	17	357.3	357.3	5.5803E-10
11	160	24	14	349.07	349.07	-3.081E-08
12	160	25	15	355.52	355.52	7.5497E-08
13	180	22	17	355.85	355.85	1.0833E-06
14	170	23	14	355.75	355.75	1.7704E-08
15	170	24	15	344.11	349.2	-5.0901318
16	170	25	16	317.48	324.6	-7.1197379
17	170	25	17	316.46	318.08	-1.62
18	170	24	14	345.6	345.6	-2.313E-08
19	160	23	15	357.14	348.422	8.71800811
20	170	22	16	355.73	355.73	8.283E-08

A time series plot illustrating the close correlation between the experimental maximum stress values and the predicted values obtained from the Artificial Neural Network (ANN) model as presented in Figure 4.6

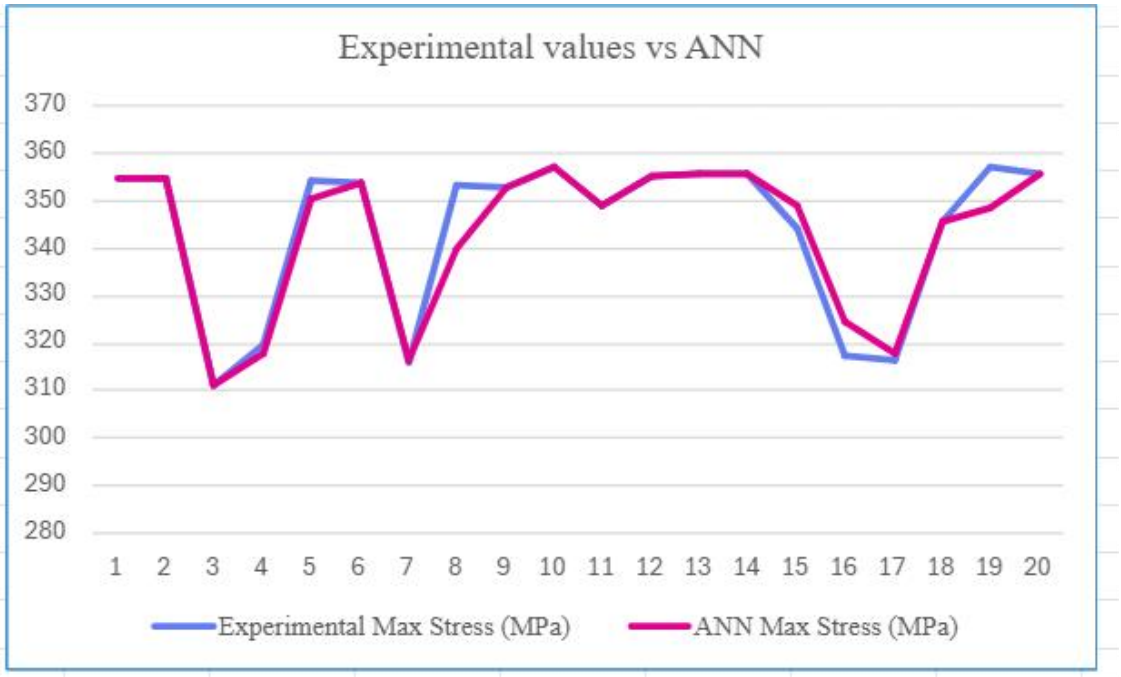

Fig 4.6: Time Series plot showing the correlation between the experimental value and ANN

The time series plot in Figure 4.6 illustrates the close correlation between the experimental maximum stress values and the predicted values obtained from the Artificial Neural Network (ANN) model. The plot shows that both data sets follow nearly identical trends across the twenty (20) data samples, indicating that the ANN model effectively captured the nonlinear relationship between the welding input parameters (current, voltage, and gas flow rate) and the resulting maximum stress. The minimal deviation between the two curves confirms that the model's predictions are consistent with the actual experimental observations. This high level of agreement

demonstrates the reliability and robustness of the developed ANN model in predicting the mechanical response of TIG weldments with a high degree of precision.

A fitted line plot further validates the strong correlation between the experimental and ANN-predicted maximum stress values as presented in Figure 4.7

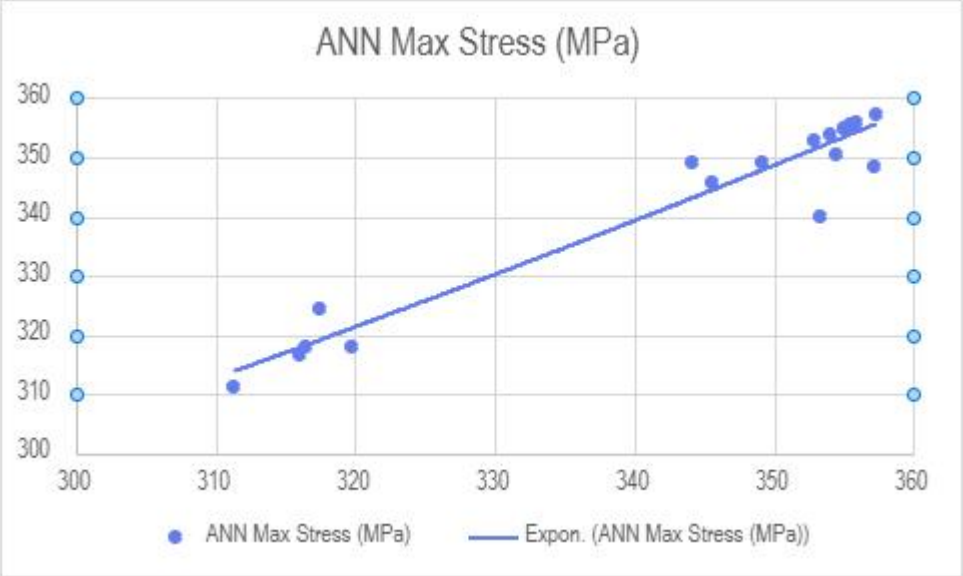

Fig 4.7: Fitted Line Plot for Actual Maximum Stress

The fitted line plot in Figure 4.7 further validates the strong correlation between the experimental and ANN-predicted maximum stress values. The plot reveals that the data points align closely along the regression line, reflecting a near-linear relationship between the predicted and actual stresses. This alignment indicates that the ANN model accurately generalised the underlying pattern in the data, maintaining predictive accuracy even for samples not directly used during training. The concentration of data points around the fitted line shows minimal error and confirms that the ANN model effectively minimized discrepancies between predicted and experimental outcomes.

4.2 DISCUSSION

In this study, welding was carried out on mild steel plate and five (5) coupons was used, the average was taking for each twenty (20) experimental runs.The CCD data was fed to the ANN to carry out prediction. The application of Artificial Neural Network (ANN) in predicting the actual maximum stress of a Tungsten Inert Gas (TIG) weldment proved to be highly effective and accurate. The developed 3–10–1 feed-forward back propagation network, using welding current, voltage, and gas flow rate as inputs, successfully captured the nonlinear relationship between these parameters and the resulting maximum stress. Through proper normalization of the data and careful selection of training algorithms and hidden neurons, the model achieved excellent performance during training. ANN to train the neural network to mark prediction for continuous response the data was set for prediction and response. Input was set for twenty (20) observations which are current, voltage and gas flow rate while the response was set for twenty (20) observation which is the actual maximum stress. The training algorithm had a random data division using the levenberg Marquardt training algorithm using mean square error (MSE) as performance determinant. The network performance value of 1.18×10^{3}, validation check of one out of six, low gradient value of 2.7276×10^{-12}, and momentum gain of 1×10^{-9} confirmed that the network was well-trained and stable, with minimal error contributions from the neurons. The regression plots revealed high correlation coefficients, with R-values of training at 99.93%,validation at 92.79%, testing at 94.40% and overall data at 96.86% indicating a strong agreement between the experimental and predicted results. The closeness of the fitted regression lines to the ideal Y=T line demonstrated the accuracy and reliability of the model. Similarly, the performance plot showed no evidence of over fitting, as the training, validation, and

testing curves followed similar trends, and best validation performance of 80.6689 at epoch 5 further validated the network's predictive capability. A comparison between the experimental and ANN-predicted maximum stress values showed only minor differences, with most errors being extremely small, confirming the high accuracy of the model. The time series and fitted line plots further established a strong correlation between experimental and predicted values, proving the model's ability to generalize beyond the training data.

Overall, the ANN demonstrated strong potential as a predictive tool for TIG welding processes, offering a reliable, efficient, and cost-effective means of estimating maximum stress without extensive experimental trials. The network's performance confirms that artificial neural networks can effectively model complex nonlinear relationships between welding parameters and mechanical responses, making them valuable for process optimization, quality control, and intelligent prediction in welding applications.

CHAPTER 5

CONCLUSION AND RECOMMENDATION

5.1 Conclusion

This study focused on the application of ANN in predicting the actual maximum stress in TIG weldment, with the aim of developing an intelligent predictive model that enhances the precision, efficiency, and safety of welded structures. The results obtained from the experimental and analytical investigations demonstrated that the ANN model effectively learned the complex relationships between the input parameters and the resulting maximum stress values confirming that Artificial Neural Networks are a reliable and robust tool for modeling the nonlinear behaviour of welding processes.

The successful application of ANN in this research demonstrates the growing relevance of machine learning and artificial intelligence in modern manufacturing and materials engineering. By integrating data-driven predictive models into welding technology, engineers can achieve improved weld quality, reduced experimental cost, and enhanced structural reliability thereby paving the way for intelligent, automated, and self-optimizing welding systems in the future.

5.2 Recommendations

Based on the findings of this study, the following recommendations are proposed:

i. Expansion of training datasets: To enhance the predictive accuracy of ANN models, future studies should include larger and more diverse experimental datasets encompassing different materials, joint configurations, and environmental conditions.

ii. Safety and training emphasis: Despite technological advances, strict adherence to welding safety procedures and proper operator training remain essential to prevent hazards and ensure quality during implementation of AI-based systems.

iii. Integration of ANN into industrial welding systems: Industries employing TIG welding should consider incorporating trained ANN models into their process control systems to enable real-time prediction and adjustment of welding parameters. This will reduce trial-and-error experimentation and improve process efficiency.

iv. Validation with additional materials: While this research focused on mild steel TIG weldments, subsequent investigations should apply the developed model to other alloys such as stainless steel, aluminum, and titanium to verify its generalization and robustness.

v. Hybrid modeling approach: Combining Artificial Neural Networks with other intelligent algorithms such as Genetic Algorithms (GA) or Adaptive Neuro-Fuzzy Inference Systems (ANFIS) is recommended for achieving multi-objective optimization of weld quality and residual stress.

vi. Real-time monitoring and control: Future research should explore the integration of ANN with sensors and feedback systems for real-time stress prediction and adaptive welding control, moving toward the implementation of smart manufacturing systems.

REFERENCE

American Welding Society (AWS). (2020). “Gas Tungsten Arc Welding (GTAW)”. *AWS Publications.*

Anderson, T. L. (2005). “Fracture Mechanics: Fundamentals and Applications” (3rd ed.). Pp 355–375..

Anderson, T. L. (2005). “Fracture Mechanics: Fundamentals and Applications”. *CRC* Pp 78 - 82.

Barlam, V., Babu, M., Vardhan, P., Ramana, V., and Chakradhar, R. (2019). “Residual stress analysis of dissimilar tungsten inert gas weldments of AISI 304 and Monel 400 by numerical simulation and experimentation”. *Journal of Materials Processing Technology*, Vol 267, Pp 241–252.

Barlam, V., Babu, M., Vardhan, P., Ramana, V., and Chakradhar, R. (2019). “Residual stress analysis of dissimilar TIG weldments of AISI 304 and Model”. *Journal of Materials Processing Technology,* Pp 34 - 42.

Basak, S., and Majumder, A. (2014). “Neural network-based modeling for weld bead geometry in TIG welding”. *Procedia Materials Science,* Vol 6, Pp 868–877.

Beer, F. P., Johnston, E. R., DeWolf, J. T., and Mazurek, D. F. (2012). “Mechanics of Materials” (6th ed.). *McGraw-Hill Education,* Pp 89-92.

Beer, F. P., Johnston, E. R., DeWolf, J. T., and Mazurek, D. F. (2012). “Mechanics of Materials” (6th ed.). *McGraw-Hill*, Pp 102-110.

Bhadeshia, H. K. D. H. (1999). “Bainite in Steels: Transformations, Microstructure, and Properties. Institute of Materials”.

Budynas, R. G., and Nisbett, J. K. (2015). “Shigley’s Mechanical Engineering Design” (10th ed.). *McGraw-Hill Education,* Pp 45 -91.

Callister, W. D., and Rethwisch, D. G. (2020). “Materials Science and Engineering: An Introduction” (10th ed.). *Wiley.*

Dally, J. W., and Riley, W. F. (1991). “Experimental Stress Analysis” (3rd ed.). *McGraw-Hill*, Pp 53–61.

Deb, K. (2001). “Multi-Objective Optimization Using Evolutionary Algorithms”.

Erhunmwunse, B. O., and Ozigagun, A. (2021). “Comparison between RSM and ANN models to predict carbon content equivalent in a TIG weld”. J*ournal of Energy Technology and Environment*, Vol 3, Pp 53–61.

Haykin, S. (1999). “Neural Networks: A Comprehensive Foundation” (2nd ed.). *Prentice Hall.*

Haykin, S. (2009). “Neural Networks and Learning Machines” (3rd ed.). *Pearson Education*, Pp 88–95.

Haykin, S. (2009). “Neural Networks and Learning Machines” (3rd ed.). *Pearson Education*, Pp 527–534.

Hibbeler, R. C. (2017). “Mechanics of Materials” (10th ed.). *Pearson Education.*

Hu, X., Pei, L., Ji, H., Yu, W., and Liu, X. (2024). “Investigation of arc voltage influence on TIG welding residual stresses”. *Journal of Manufacturing Processes*, Vol 102, Pp 88–95.

Jeffus, L. (2012). “Welding: Principles and Applications” (8th ed.). *Delmar Cengage Learning.*

Kalpakjian, S., and Schmid, S. R. (2014). “Manufacturing Engineering and Technology” (7th ed.). *Pearson.*

Kannan, T., Senthilkumar, V., and Ramasamy, R. (2018). “Optimization of TIG welding parameters using response surface methodology”. *Procedia Manufacturing,* Vol 20, Pp 527–534.

Khan, M., Junaid, M., Baig, M., and Haider, S. (2019). “Response surface approach to minimise the residual stresses in full penetration pulsed TIG weldments of Ti-5Al-2.5Sn alloy”. *Journal of Manufacturing Processes*, Vol 44, Pp 287–297.

Kim, I. S., Basu, A., and Jung, Y. S. (2005). “Prediction of tensile strength in gas tungsten arc welding by artificial neural network. Materials and Design” Vol 26, Pp 609–616.

Kou, S. (2003). “Welding Metallurgy” (2nd ed.). *Wiley-Interscience.*

Kutelu, B., Seidu, E., Eghabor, E., and Ibitoye, F. (2018). “Influence of TIG welding speed and current on residual stresses in mild steel weldments”. *Engineering Research Journal,* Vol 5(2), Pp 115–124.

Liu, Y., and Alton, D. (2000). “Analysis of welding distortion and residual stress”. *International Journal of Pressure Vessels and Piping*. Vol 77(10), Pp 681–687.

Logan, D. L. (2016). “A First Course in the Finite Element Method” (6th ed.). *Cengage Learning*.

Marinelli, G., Martina, F., Ganguly, S., and Williams, S. W. (2019). “The effect of shielding gas composition on arc characteristics and weld quality in TIG welding”. *Welding Journal*, Vol. 98, Pp. 128–139.

Megson, T. H. G. (2014). “Aircraft Structures for Engineering Students” (6th ed.). *Butterworth-Heinemann*.

Minh, N. T., Nguyen, H. L., Do, M. H., Uyen, T. V., Toan, N. H., Linh, V. T., and Nguyen, D. H. (2024). “Analysis of current and voltage influence on residual stress in TIG welding of stainless steel”. Vol 94, Pp 364–371.

Mishurova, T., et al. (2022). “Residual stress characterization in TIG-welded steel by combined neutron and X-ray diffraction”. *Journal of Applied Crystallography*, Vol. 55, Pp. 332–341.

Montgomery, D. C. (2017). “Design and Analysis of Experiments” (9th ed.). *Wiley.*

Palani, P. K., and Murugan, N. (2006). “Development of mathematical models for prediction of weld bead geometry in TIG welding of stainless steel”. *Journal of Materials Processing Technology*, Vol 176, Pp 167–174.

Parikin, P., Nurlina, I., and Basori, M. (2017). “Residual stress evaluation on TIG welds in 57Fe-15Cr-25Ni steel using X-ray diffraction”. *Materials Science Forum*, Vol 90, Pp 93–99.

Patil, S. M., and Suryawanshi, J. G. (2020). “Prediction of residual stress in TIG welding using artificial neural network”. Vol 26, Pp 315–321.

Prime, M. B. (2001). “Cross-sectional mapping of residual stresses by measuring the surface contour after a cut”. *Journal of Engineering Materials and Technology*, Vol 123(2), Pp 162–168.

Ravichandran, M., Kumar, S., and Arivazhagan, N. (2015). “Optimization of welding parameters for TIG welding using genetic algorithm”. *International Journal of Advanced Manufacturing Technology,* Vol 77, Pp 327–335.

Schajer, G. S. (2010). “Practical Residual Stress Measurement Methods”. *Wiley.*

Sindo, K., and Hosseini, M. (2019). “Welding Principles and Applications”.

Springer, M. T. (2025). “Review of residual stress effects in carbon steel weldments”. *International Journal of Advanced Welding Science,* Vol 11(1), Pp 15–32.

Totten, G. E., and Howes, M. A. H. (1997). “Steel Heat Treatment Handbook”. *CRC Press.*

Totten, G. E., Howes, M. A. H., and Inoue, T. (2002). “Handbook of Residual Stress and Deformation of Steel”. *ASM International.*

Webster, P. J., Ananthavaravakumar, M., and Withers, P. J. (2002). “Residual stress measurement in welded structures by neutron diffraction”. *Applied Physics* Vol 74(1), Pp 179–182.

Withers, P. J., and Bhadeshia, H. K. D. H. (2001). “Residual stress. Part 1: Measurement techniques”. *Materials Science and Technology,* Vol 17(4), Pp 355–365.

Withers, P. J., and Bhadeshia, H. K. D. H. (2001). “Residual stress: Part 1 – Measurement techniques; Part 2 – Nature and origins”. *Materials Science and Technology*, Vol 17, Pp 355–375.

Zhang, Y., Chen, J., and Fang, Y. (2017). “Applications of artificial neural networks in welding technology”. *International Journal of Advanced Manufacturing Technology*, Vol 90, Pp 1975–1987.

Zhao, Z., Liu, S., and Wang, X. (2019). “Prediction of weld bead geometry using SVM and random forest algorithms”. *Procedia Manufacturing,* Vol 35, Pp 1245–1253.